Molecular rearrangements of diynes coordinated to triosmium carbonyl clusters: the synthesis and structural characterisation of [Os$_3$(μ-H)(CO)$_{10}$\{μ$_3$-η^1:η^3:η^1-Ph(C)C$_9$H$_6$)\}], [Os$_3$(μ-H)(CO)$_9$\{μ$_3$-η^1:η^3:η^1-Ph(C)C$_9$H$_6$)\}] and [Os$_3$(μ-H)(CO)$_8$(MeCN)\{μ$_3$-η^1:η^3:η^1-Ph(C)C$_9$H$_6$)\}]

Lionel P. Clarke [a], John E. Davies [a], Dmitrii V. Krupenya [b], Paul R. Raithby [a,1,*], Gregory P. Shields [a], Galina L. Starova [b], Sergey P. Tunik [b,*]

[a] Department of Chemistry, Lensfield Road, Cambridge CB2 1EW, UK
[b] Department of Chemistry, St. Petersburg University, Universitetskii pr., 2, St. Petersburg 198904, Russian Federation

Abstract

The reaction between [Os$_3$H$_2$(CO)$_{10}$] and 1,4-diphenylbuta-1,3-diyne yields two isomers of the triosmium cluster [Os$_3$(μ-H)(CO)$_{10}$\{μ$_3$-η^1:η^3:η^1-Ph(C)C$_9$H$_6$)\}] **1**, **2**, the structures of which involve an 'open' metal triangle and exhibit an unusual pseudo-allylic interaction involving a fused six- and five-membered ring system obtained from a ring-closure reaction of the diyne. Thermal decarbonylation of **1** and **2** produces [Os$_3$(μ-H)(CO)$_9$\{μ$_3$-η^1:η^3:η^1-Ph(C)C$_9$H$_6$)\}] (**3**) which has a 'closed' Os$_3$ triangular core and the same formal μ$_3$-η^1:η^3:η^1-allylic coordination mode. The reaction of **1** with trimethylamine-N-oxide in the presence of acetonitrile affords [Os$_3$(μ-H)(CO)$_8$(MeCN)\{μ$_3$-η^1:η^3:η^1-(Ph(C)C$_9$H$_6$)\}] (**4**), an acetonitrile-substituted derivative of **3**. The structures of clusters **1**–**4** have been established by X-ray crystallography, and all the new clusters have been characterised spectroscopically.
© 2003 Elsevier B.V. All rights reserved.

Keywords: Osmium; Diyne; Carbonyl cluster; X-ray crystal structures; NMR

1. Introduction

The chemistry of alkynes when coordinated to transition-metal carbonyl clusters is well documented [1–7]. Alkynes display a wide range of coordination modes when coordinated to polynuclear carbonyl clusters, and their reactivity is characterised by transition-metal mediated carbon–carbon bond formation and cyclizations of unsaturated hydrocarbons [5–7]. More recently, the reactions of 1,3-conjugated diynes with ruthenium and osmium clusters have attracted considerable interest because of the unusual transformations that these molecules undergo when they are attached to the cluster core. For the osmium systems observed chemistry includes intramolecular rearrangement/cyclization of the ligand under mild conditions [8–12] and carbon–carbon rupture in thermolysis reactions [13], and related results are observed for ruthenium cluster systems [14]. The result of the ligand rearrangement generally depends essentially on the nature of terminal substituents of the diyne. When the reaction involves the use of [Os$_3$H$_2$(CO)$_{10}$], a hydrogen atom attached to the β-carbon atom of the diyne substituent may be abstracted, and this leads to the formation of a bond between the β-carbon atom and the third carbon (relative to the substituent) of the –C$_2$–C$_2$– diyne group [12]. Here, we report the reaction of [Os$_3$H$_2$(CO)$_{10}$] and 1,4-diphenylbuta-1,3-diyne that involves the generation of

---

* Corresponding authors. Fax: +44-1225-38-3183 (P.R.R).
  E-mail address: p.r.raithby@bath.ac.uk (P.R. Raithby).
[1] Present address: Department of Chemistry, University of Bath, Claverton Down, Bath BA2 7AY, UK.

an unusual pseudo-allylic ligand that contains a fused six- and five-membered ring system.

2. Results and discussion

The reaction of $[Os_3H_2(CO)_{10}]$ with 1,4-diphenylbuta-1,3-diyne, in chloroform, at room temperature for 18 h, affords three compounds after separation by TLC using hexane/dichloromethane (6:1) as eluant. The main yellow, air stable product **1** was obtained in 50% yield (high R_f), and was characterised as an isomer of $[Os_3(\mu\text{-}H)(CO)_{10}\{\mu_3\text{-}\eta^1\text{:}\eta^3\text{:}\eta^1\text{-}(Ph(C)C_9H_6)\}]$ by spectroscopic (Tables 1 and 2) and crystallographic methods. The second product, **2**, characterised as a second isomer of $[Os_3(\mu\text{-}H)(CO)_{10}\{\mu_3\text{-}\eta^1\text{:}\eta^3\text{:}\eta^1\text{-}(Ph(C)C_9H_6)\}]$ was obtained as an orange solid in 25% yield (low R_f). Small amounts of the known complex $[Os_3(CO)_{10}\{PhC_2C_2Ph\}]$ (**5**) were also obtained upon purification. This complex was characterised by mass spectrometry (molecular ion $m/z = 1052$), and by comparison of the IR and ^1H-NMR spectra with the literature data [15,16].

The FAB mass spectra of **1** and **2** both gave the same molecular ion peak at m/z 1054, followed by sequential mass losses corresponding to the removal of ten carbonyl ligands. The IR spectra of the two complexes in the carbonyl region (Table 1) showed significant differences, consistent with a change in molecular symmetry. The ^1H-NMR spectra for each compound indicated the presence of a hydride ligand, nine protons in the aromatic region, and a methylene group. How-

ever, there were significant differences in the positions of the hydride and methylene signals. All these observations were consistent with the fact that **1** and **2** were structural isomers. In order to establish the metal and ligand arrangements the molecular and crystal structures were determined by single-crystal X-ray analyses.

Stable single crystals of **1** were grown from dichloromethane/hexane solution at $-30\,^\circ C$. These crystals were shown to crystallise in the triclinic space group $P\bar{1}$ (No. 2). Under different crystallisation conditions, a chloroform/heptane solution at $-5\,^\circ C$, a different polymorph, with space group $C2/c$, was obtained. The gross features of the molecular structure were the same in both polymorphs and only those for the triclinic form, denoted **1a**, will be discussed in detail. Crystallographic data for the monoclinic form, denoted **1b**, has been deposited as supplementary crystallographic data. Single crystals of **2** were obtained by recrystallisation from dichloromethane/hexane solution at $-30\,^\circ C$.

The crystal structures of **1a** and **2** consist of discrete $[Os_3(\mu\text{-}H)(CO)_{10}\{\mu_3\text{-}\eta^1\text{:}\eta^3\text{:}\eta^1\text{-}(Ph(C)C_9H_6)\}]$ molecules with no abnormally short intermolecular contacts. For **1a** two crystallographically independent but structurally similar molecules are present in the asymmetric unit. The molecular structures of **1a** and **2** are shown in Figs. 1 and 2, respectively, while selected bond parameters are listed in Tables 3 and 4. The X-ray analyses confirm that **1a** and **2** are isomeric structures, the most significant structural differences being the orientation of the indane-2-yl-1-ylidene, $(Ph(C)C_9H_6)$, ligand over the open Os_3 triangle, and the relative position of the edge-bridging hydride with respect to the organic ligand.

Table 1
Spectroscopic data for compounds **1**–**5**

Compound	ν(CO) (cm^{-1})	Colour	Mass spectroscopy [a]	^1H-NMR (δ, J/Hz) [b,c]
1	[d] 2110(w), 2080(s), 2072(w), 2060(vs),2028(vs), 2006(s), 1984(m), 1960(w)	Yellow	1054 (1054) $Os_3 = (570)$	[b] 7.90–6.27 (m, 9H, six-mem. rings) 3.63 (s, 2H, CH_2), -16.84 (s, 1H, μ-HOs).
2	[b] 2100(m), 2081(s), 2066(vs), 2050(vs), 2023(m), 1997(sh)	Yellow	1054 (1054) $Os_3 = (570)$	[b] 7.60–6.76 (m, 9H, six-mem. rings) 4.40 (AA′, 2H, CH_2, $J = 21.7$ Hz), -17.34 (s, 1H, μ-HOs).
3	[d] 2096(s), 2072(vs), 2046(vs), 2020(s), 2004(vs), 1988(w)	Yellow	1026 (1026) $Os_3 = (570)$	[b] 7.70–5.87 (m, 9H, six-mem. rings), 3.66 (AA′, 2H, CH_2, $J = 21.0$ Hz), -18.37 (s, 1H, μ-HOs).
4	[b] 2082(s), 2060(s), 2056(sh), 2035(m), 2009(sh), 1995(vs), 1981(sh), 1941(m)	Yellow	1039 (1039) $Os_3 = (570)$	[c] 7.65–6.03 (m, 9H, six-mem. rings), 3.58 (AA′, 2H, C$_{H_2}$, $J = 21.9$ Hz), 1.93 (s, 3H, CH_3CN), -17.85 (s, 1H, μ-HOs).
5	[d] 2084(s), 2072(s), 2060(m), 2036(m), 2028(vs), 2016(s), 2004(w), 1994(w)	Yellow	1052 (1052) $Os_3 = (570)$	[b] 7.55–7.30 (m, 10H Ph),

[a] Molecular ion and the signals corresponding to successive loss of CO ligands (ten CO (**1**), (**2**) and (**5**), nine (**3**), eight (**4**)) were observed. Calculated values are in parentheses.
[b] CDCl$_3$.
[c] CD$_2$Cl$_2$.
[d] Hexane.

Table 2
Spectroscopic data for compounds **1**–**4**

Compound	Analysis (C, H, N) [a]	^{13}C-NMR, δ ppm, (multiplicity, assignment)
1	C—29.28 (29.57); H—1.08 (1.11)	187.5–166.6 (10s, 10C, 10 CO), 151.4, 150.3, 148.6, 141.8 (4s, 4C), 129.7–123.8 (9s, 9CH, six-mem. rings), 101.9 (s, 1C), 59.7 (s, 1C, CH_2), 23.6 (s, 1C) [b]
2	C—28.94 (29.57); H—1.15 (1.11)	189.7–166.7 (10s, 10C, 10 CO), 158.3, 151.6, 144.0, 140.8 (4s, 4C), 128.0–124.2 (9s, 9CH, six-mem. rings), 106.3 (s, 1C), 51.7 (s, 1C, CH_2), 22.8 (s, 1C) [b]
3	C—30.19 (30.00); H—1.48 (1.20)	174.57 (s, 9C, 9 CO), 158.25,155.47, 152.46 (3s, 3C), 149.50 (s, 1C), 142.99 (s, 1C), (s, 1C,), 129.9–123.9 (7s, 9CH, six-mem. rings), 55.11 (s, 1C, CH_2) [c]
4	C—30.15 (30.00); H—1.85 (1.76); N—0.73.(1.3)	178.35 (s, 8C, 8 CO), 132.45–126.80 (7s, 9C, Ph/six-mem. ring), 55.80 (s, 1C, CH_2), 42.24 (s, 1C, CH_3CN) [c,d]

[a] Calculated values in parentheses.
[b] CDCl$_3$.
[c] CD$_2$Cl$_2$.
[d] Poor resolution precludes complete assignment.

In both the structures of **1a** and **2** the three osmium atoms adopt an open triangular arrangement with one Os···Os edge lengthened to 3.766(2) Å [3.755 (2) Å for the second independent molecule] for **1a** and 3.733(2) Å for **2**. This distance may be viewed as non-bonding, consistent with the overall electron count of 50 e$^-$ for both clusters assuming that the substituted indene ligand acts as a 5 e$^-$ donor. In each structure the two Os–Os bonds show significant differences in length, but this is consistent with the presence of a bridging hydride spanning the longer edge in each case; the edge lengthening effect of a bridging hydride is well estab-

lished [17]. In both the structures of **1a** and **2** the hydride positions were not located directly but they were derived from potential energy calculations [18,19].

Again, in both the structures of **1a** and **2**, the ten carbonyl ligands adopt terminal sites and are essentially linear. One of the 'terminal' Os atoms has four carbonyls, two in axial and two in equatorial sites, and the other 'terminal' Os and the 'linking' Os atom in the open triangle have three carbonyls coordinated to them.

The most interesting feature of the structures of **1a** and **2** is the nature of the coordinated (Ph(C)C$_9$H$_6$) ligand that is formed from the original 1,4-diphenyl-
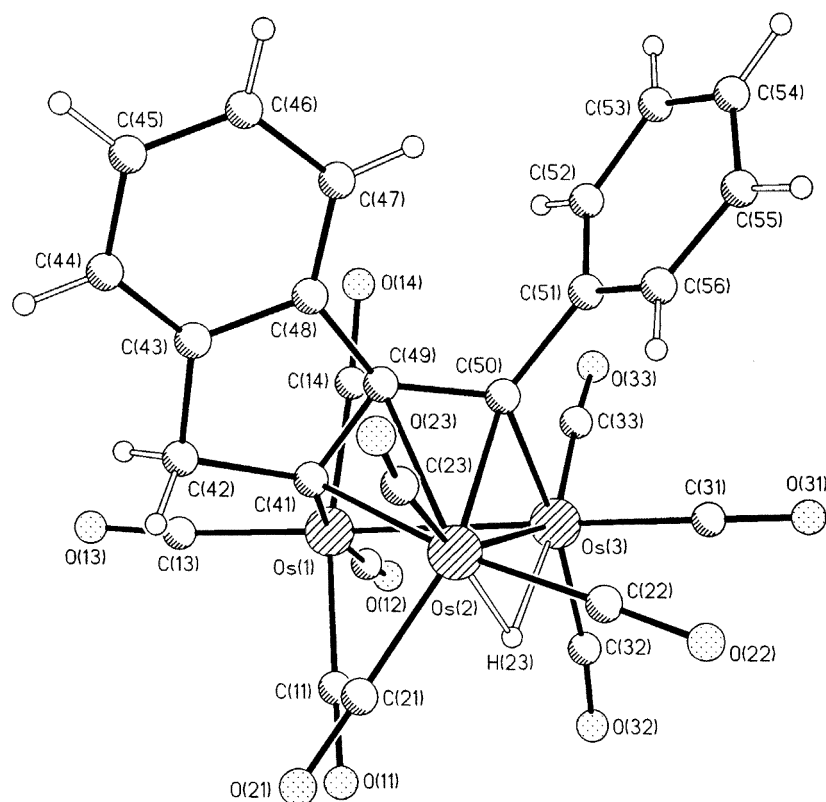

Fig. 1. The molecular structure of one of the two independent molecules of **1a** showing the atom numbering scheme adopted.
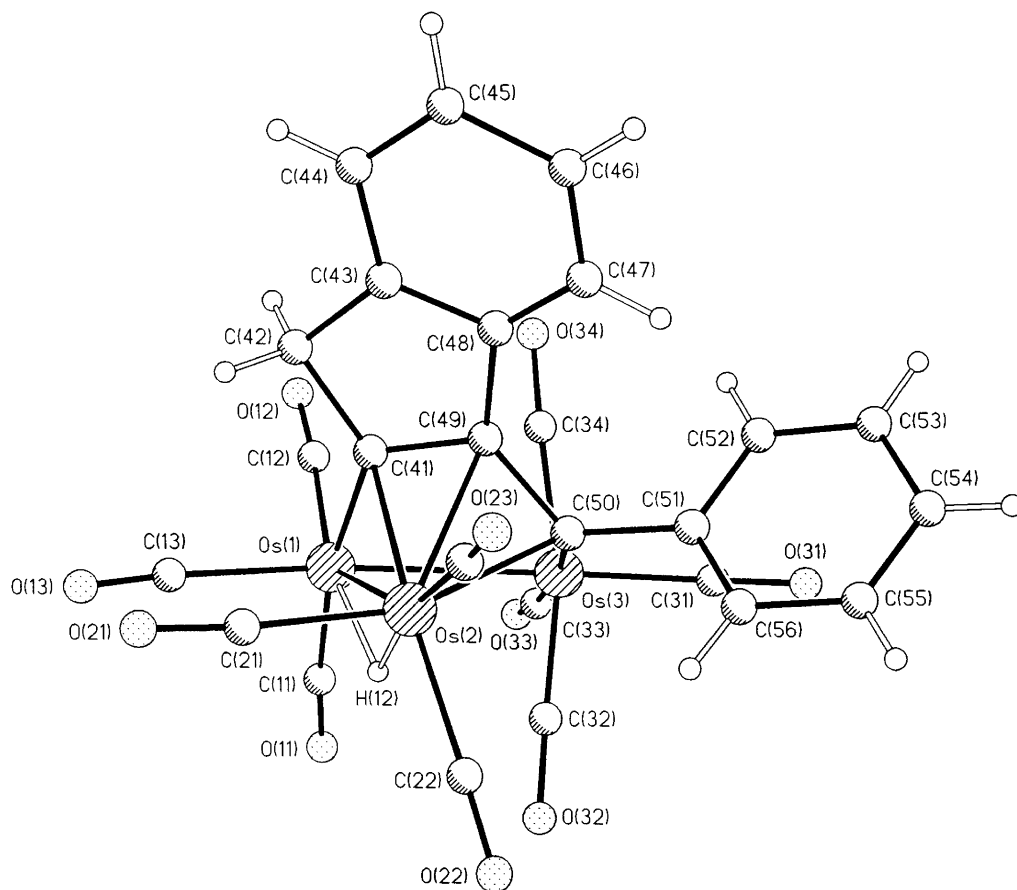
Fig. 2. The molecular structure of **2** showing the atom numbering scheme adopted.

buta-1,3-diyne by a cyclization process coupled with the transfer of two hydrogen atoms onto the unsaturated –C≡C–C≡C– hydrocarbon chain. It is probable that one of these hydrogen atoms derives from $[Os_3H_2(CO)_{10}]$ and the other is transferred from the C(48) atom (see Fig. 1). This transfer is accompanied by C–C bond formation between the phenyl carbon C(48) and the C(49) atom of the diyne chain. The resultant $(Ph(C)C_9H_6)$ ligand then bridges all three osmium atoms, and can be viewed as forming a pseudo-allylic interaction with Os(2) (Figs. 1 and 2) and σ-interactions with Os(1) and Os(3), thus providing 5 e$^-$ towards the cluster electron count. The difference between the two isomeric structures is that in **1a** the indenyl ligand spans the open Os···Os edge, such that C(41) may be viewed as having inserted into the Os(1)–Os(2) bond, and the phenyl substituent and the associated C(50) atom bridge the Os(2)–Os(3) edge that is also spanned by the bridging hydride. In **2** the phenyl substituent and associated C(50) atom span the open Os(2)···Os(3) edge, with C(50) having inserted into the metal–metal bond, and the indenyl, through C(41), spans the hydride-bridged Os(1)–Os(2) edge. In **1a** the C(41)–C(49) and C(49)–C(50) lengths of 1.42(4) [1.39(3)] and 1.41(3) [1.36(3)] Å, respectively, are consistent with the

allylic description of the bonding, and the C(49)–C(50)–C(51) and C(41)–C(49)–C(50) bond angles are close to the expected value of 120°. The angles around C(41) are closer to tetrahedral, and it is possible that there is a greater σ-bonding component in the bond between C(41) and Os(2). In **2** the C(41)–C(49) and C(49)–C(50) bonds, with distances of 1.43(2) and 1.50(2) Å show a greater variation in length, but the angles about C(41), C(49) and C(50) are very similar to those in **1a**.

The X-ray structure determinations of **1a** and **2** are consistent with the differences in the ^{1}H-NMR data for the two clusters. The hydride signals for **1** and **2** (Table 1) are both indicative of edge bridging hydrides but the small difference in the positions of the signals reflects the difference in their environments. In **1** the methylene protons appear as a singlet at δ 3.66, indicating that while they are not chemically equivalent by symmetry, they are coincidently appear at the same position because of their similar environments. In contrast, in **2**, from the asymmetry in the structure, the two methylene protons are clearly in different environments and consequently appear as an AA' signal centred at δ 4.40 with $J_{HH} = 21.7$ Hz.

The room temperature ^{13}C-NMR spectrum of **1** (Table 2) exhibits ten resolved resonances for the carbon

Table 3
Selected bond lengths (Å) for compounds **1a**, **2**, **3** and **4**

|	**1a**	**2**	**3**	**4**
Os(1)–Os(3)	2.857(2), 2.859(2)	2.8548(10)	2.9601(11), 2.9446(11)	2.9601(9)
Os(2)–Os(3)	2.894(2), 2.890(2)	–	2.8349(11), 2.8271(11)	2.8084(8)
Os(1)–Os(2)	–	2.9379(11)	2.8365(10), 2.8460(10)	2.7925(8)
Os(1)–C(41)	2.16(3), 2.23(3)	2.06(2)	2.27(2), 2.10(2)	2.08(2)
Os(3)–C(50)	2.17(2), 2.27(3)	2.16(2)	2.11(2), 2.16(2)	2.105(13)
Os(2)–C(41)	2.30(3), 2.33(3)	2.25(2)	2.27(2), 2.24(2)	2.317(14)
Os(2)–C(49)	2.27(2), 2.24(2)	2.262(14)	2.28(2), 2.29(2)	2.361(13)
Os(2)–C(50)	2.17(2), 2.24(3)	2.32(2)	2.29(2), 2.28(2)	2.264(12)
C(41)–C(42)	1.61(4), 1.53(3)	1.56(2)	1.53(2), 1.63(2)	1.55(2)
C(42)–C(43)	1.50(4), 1.49(3)	1.54(2)	1.47(3), 1.50(3)	1.49(2)
C(43)–C(48)	1.38(4), 1.37(3)	1.36(2)	1.43(3), 1.35(3)	1.38(2)
C(48)–C(49)	1.49(3), 1.50(3)	1.56(2)	1.49(2), 1.52(2)	1.48(2)
C(41)–C(49)	1.42(4), 1.39(3)	1.43(2)	1.38(2), 1.31(2)	1.45(2)
C(49)–C(50)	1.41(3), 1.36(3)	1.50(2)	1.42(2), 1.33(2)	1.43(2)
C(50)–C(51)	1.54(3), 1.44(3)	1.55(2)	1.53(2), 1.53(2)	1.53(2)
Os(2)–N(1)	–	–	–	2.093(12)
N(1)–C(2)	–	–	–	1.14(2)
C(2)–C(3)	–	–	–	1.43(2)

atoms of the carbonyl groups, consistent with the complete asymmetry of the carbonyl environments within this molecule. This result also indicates that the molecule is stereochemically rigid at this temperature. On the basis of a DEPT 135 experiment the high field

signal at 60.07 ppm can be assigned to the methylene carbon, C(42), and the set of nine well resolved resonances (129.7–123.9 ppm) to the carbon atoms of the aromatic rings that are bound to hydrogens, C(44)–C(47) and C(52)–C(56). The other six resonances observed in the spectrum correspond to the 'bare' carbon atoms of the coordinated ligand. It is not possible to make unambiguous assignments for these signals. The signal at 23.6 ppm is unusually high, and according to the results of the DEPT 135 experiment, this resonance with zero intensity in the DEPT spectrum has to be assigned to a 'metal-bound' carbon. The ^{13}C-NMR spectrum of **2** (Table 2) is very similar to that of **1**, including a high field signal at 22.8 ppm, and similar assignments of the resonances can be made. This is as expected for two isomers with quite similar structures.

The course of the reaction between $[Os_3H_2(CO)_{10}]$ and 1,4-dipehnylbuta-1,3-diyne was monitored by ^{1}H-NMR spectroscopy in order to gain information regarding the mechanism of the process. In the experiment the reaction mixture, in CD_2Cl_2, was placed in an NMR tube and the changes in the hydride signals from $[Os_3H_2(CO)_{10}]$ (δ −11.5), 1 (δ −16.8) and 2 (δ −17.3) were monitored. At room temperature consumption of the dihydride and formation of the three products, **1**, **2** and $[Os_3(CO)_{10}(PhC_2C_2Ph)]$ (**5**) occurred at an equal rate of 0.017 ± 0.002 min^{-1}. This indicates that all the products obtained originate from a common intermediate, the stage at which it is formed being the rate-determining step for the reaction. A possible reaction sequence that is consistent both with the structural data obtained for the products as well as with the assumption of a common alkenyl intermediate is illustrated in Scheme 1, although no attempt was made to isolate organic products generated in the reaction. The first step in the process has been observed frequently in the interaction between alkynes and $[Os_3H_2(CO)_{10}]$, and alkenyl intermediates of this type have been isolated and characterised for various alkynes

Table 4
Selected bond angles (°) for compounds **1a**, **2**, **3** and **4**

	1a	**2**	**3**	**4**
Os(1)–Os(3)–Os(2)	81.81(6), 81.55(6)	–	58.56(3), 59.05(3)	57.83(2)
Os(2)–Os(1)–Os(3)	–	80.24(3)	58.51(2), 58.42(3)	58.36(2)
Os(1)–Os(2)–Os(3)	–	–	62.92(3), 62.54(3)	63.81(2)
Os(1)–C(41)–Os(2)	115.3(12), 110.7(11)	85.9(6)	81.3(6), 81.9(6)	78.7(5)
Os(3)–C(50)–Os(2)	83.7(8), 79.7(9)	112.8(8)	80.0(5), 79.0(6)	79.9(4)
C(41)–C(42)–C(43)	103(2), 104(2)	100.5(14)	106(2), 100(2)	104.4(12)
C(42)–C(41)–C(49)	106(2), 110(2)	108.2(13)	106.6(14), 109(2)	107.0(13)
C(41)–C(49)–C(50)	117(2), 126(2)	117.0(13)	120(2), 121(2)	120.6(12)
C(41)–C(49)–C(48)	111(2), 106(2)	110.8(12)	112(2), 110(2)	107.9(12)
C(49)–C(50)–C(51)	120(2), 120(2)	116.0(14)	117.6(14), 123(2)	117.5(11)
Os(2)–N(1)–C(2)	–	–	–	175.5(12)
N(1)–C(2)–C(3)	–	–	–	178(2)

Scheme 1.
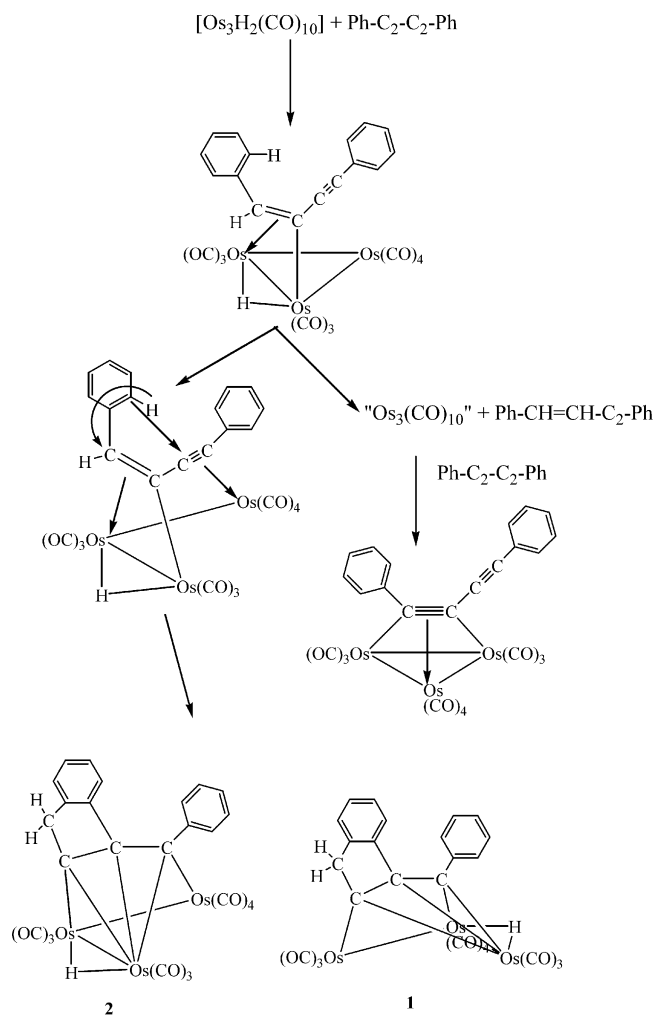
[20,21]. In the case of the reaction with the diyne it is evident that this intermediate is highly reactive and undergoes further transformations [10–12]. For example, in the reaction with 1,4-bis(trimethylsilyl)diyne, the alkenyl coordination mode is stabilised by a 1,2 silyl shift [12]. One possible path is the intramolecular cyclization process leading to the formation of **1** and **2**. In an alternative pathway, the second hydride is transferred on to the coordinated ligand resulting in the expulsion of an enyne and the further reaction of the unsaturated 'Os$_3$(CO)$_{10}$' fragment with another diyne molecule to give [Os$_3$(CO)$_{10}$(PhC$_2$C$_2$Ph)]. A similar reaction sequence was monitored in detail for the reaction between [Os$_3$H$_2$(CO)$_{10}$] and diphenylacetylene [3].

Thermolysis of either a mixture of **1** and **2** or of the individual isomers, in heptane, for 3 h, followed by separation and purification by TLC using hexane as eluant, affords a single yellow product in 90% yield (Scheme 2). This product was characterised as [Os$_3$(μ-H)(CO)$_9${μ$_3$-η^1:η^3:η^1-(Ph(C)C$_9$H$_6$)}] (**3**) by IR, ^{1}H- and

^{13}C-NMR spectroscopies, FAB mass spectrometry (Tables 1 and 2), and the analysis was confirmed by a single-crystal X-ray diffraction study.

The mass spectrum for **3** gives a molecular ion at *m/z* 1026 and also shows the sequential loss of nine carbonyl ligands. This observation is consistent with the removal of one carbonyl ligand from **1** and **2** during the thermolysis reaction to produce the complex **3** that contains nine carbonyl ligands. This is confirmed by the X-ray analysis. The crystal structure of **3** contains two independent but structurally similar molecules in the asymmetric unit. The molecular structure of one of these molecules is shown in Fig. 3 while selected bond parameters are listed in Tables 3 and 4. The metal framework in **3** consists of a closed, ca. isosceles triangle the longest edge [Os(1)–Os(3)] of which is bridged by a hydride ligand. As with the structures of **1** and **2** the hydride position was assigned from potential energy calculations [19]. The nine carbonyl ligands are all terminal and essentially linear. Three carbonyls are coordinated to each Os atom, two in equatorial and one in an axial site; in one of the independent molecules three of the carbonyl groups show positional disorder over two sites and the positions were refined with partial occupancies that summed to unity. The indane-2-yl-1-ylidene ligand retains the μ$_3$-η^1:η^3:η^1-coordination mode to the metal framework, with an η^3-allylic interaction to Os(2), and σ-interactions between Os(1)–C(41) and Os(3)–C(50), to give a pentagonal pyramidal Os$_3$C$_3$ cluster core. However, unlike the coordination of this ligand in **1** and **2**, the metal–ligand distances are significantly more asymmetric. The C(41)–C(49) and C(49)–C(50) distances lie in the same range as those found in **1a** and **2**, and the angles at the allylic carbon atoms are also similar.

In terms of electron counting, the organic ligand in **3** still acts as a 5 e$^-$ donor, and with the loss of a carbonyl compared to **1** or **2**, the overall count is reduced to 48 e$^-$. This is the expected count for a closed triangular metal framework, so that the loss of a carbonyl is concomitant with the closing of the open metal triangle observed in **1** and **2**.

The ^{1}H- and ^{13}C-NMR data presented in Tables 1 and 2 is consistent with the solid state structure of **3**. As in the case of **1** and **2** a multiplet of nine protons corresponding to the aromatic protons is observed in the range δ 7.9–5.8 in the ^{1}H-NMR spectrum at room temperature. The methylene protons display an *AA′* signal centred at δ 3.66 and the resonance for the bridging hydride appears at δ −18.38. In the room temperature ^{13}C-NMR spectrum of **3** one resonance of relative intensity nine is observed in the carbonyl region (174.57 ppm). This suggests that this complex is completely stereochemically nonrigid at room temperature and all nine carbonyls take part in the scrambling around the Os$_3$ triangle. This is in complete contrast to
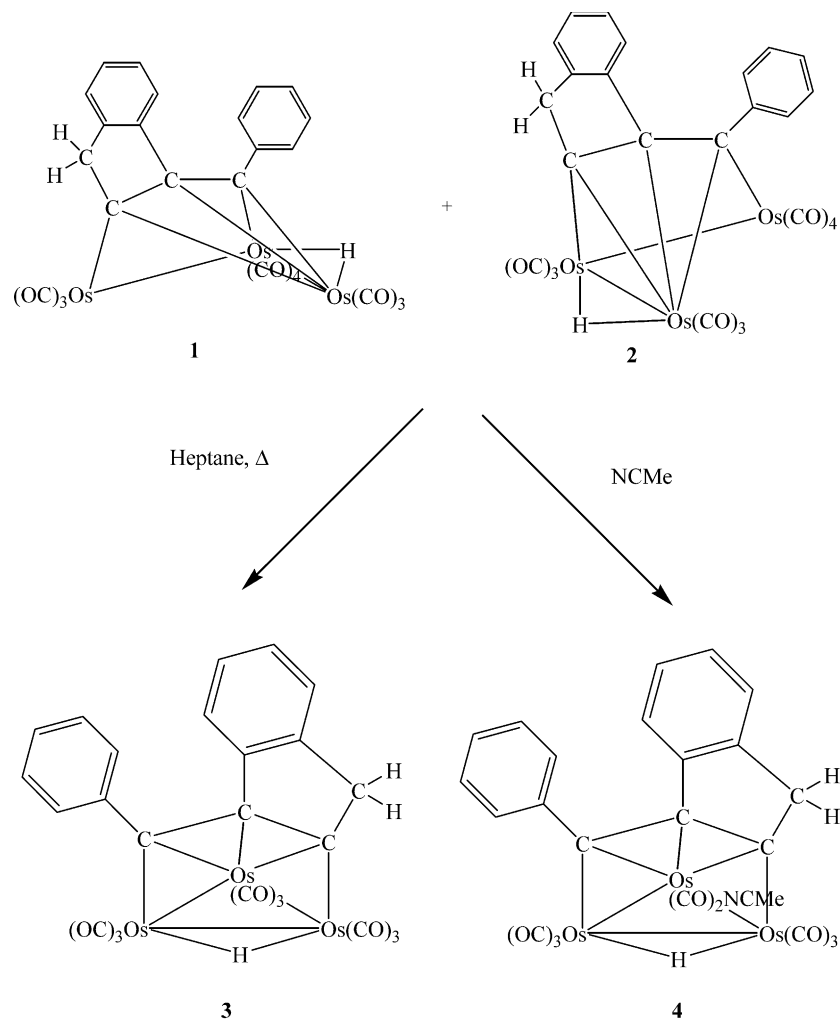
Scheme 2.

the stereochemically rigid carbonyls in **1** and **2**. The difference in dynamic behaviour may be attributed to the difference in the metal framework between **1** and **2** and **3**. The open triangle in **1** and **2** prevents carbonyl scrambling over the metal framework, whereas, in **3**, the 'merry-go-round' mechanism over the closed triangle is evidently responsible for the observed behaviour. The remaining ^{13}C assignments (Table 2), for the organic ligand in **3**, are similar to those described for **1** and **2**, except that the very high field signal expected at around 23 ppm, ascribed to a 'metal bound' carbon could not be located. The poor solubility of **3** in organic solvents at lower temperatures prevented a more detailed interpretation of the ^{13}C-NMR spectrum.

The reaction of $[Os_3(\mu\text{-H})(CO)_{10}\{\mu_3\text{-}\eta^1:\eta^3:\eta^1\text{-}Ph(C)C_9H_6)\}]$ (**1**) with 1.2 equivalents of trimethylamine-n-oxide in a CH_2Cl_2–acetonitrile solution affords an acetonitrile derivative of **3** $[Os_3(\mu\text{-}H)(CO)_8(MeCN)\{\mu_3\text{-}\eta^1:\eta^3:\eta^1\text{-}Ph(C)C_9H_6)\}]$ (**4**). The complex has been characterised by spectroscopic tech-

niques (Tables 1 and 2) and by an X-ray analysis. The molecular structure of **4** is shown in Fig. 4 while selected bond parameters are listed in Tables 3 and 4. The metal framework geometry of **4** is very similar to that of **3**. The acetonitrile ligand is linearly bonded to Os(2) which is η^3-coordinated to the allylic moiety. The acetonitrile occupies a pseudo-axial site, as is observed in $[Os_3(CO)_{10}(NCMe)_2]$ [22], because on electronic grounds it is favourable for this ligand to be *trans* to a carbonyl ligand rather than *trans* to a metal–metal edge. The bond parameters for the organic ligand coordination are also closely similar to those in **3**. The spectroscopic data is similar to that observed for **3** except for an additional signal at δ 1.93 in the ^{1}H-NMR spectrum corresponding to the methyl group of the acetonitrile ligand, with only one CO resonance in the ^{31}C-NMR spectrum indicating CO scrambling at room temperature. The mass spectrum displayed the molecular ion peak at *m/z* 1039, and the sequential loss of the acetonitrile ligand and eight carbonyl groups.
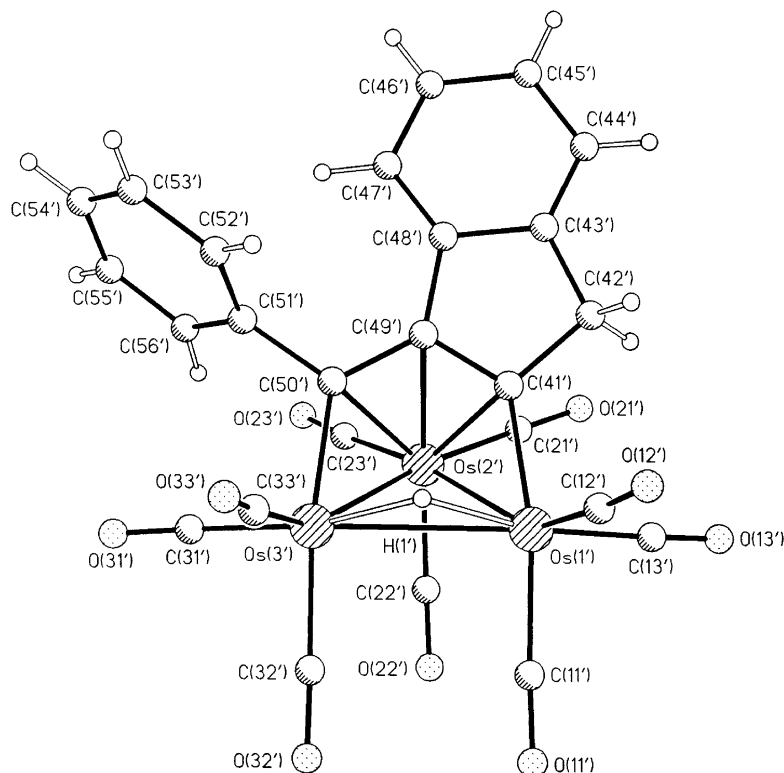
Fig. 3. The molecular structure of one of the two independent molecules of **3** showing the atom numbering scheme adopted.

3. Experimental

All the reactions were performed using standard Schlenk techniques under an atmosphere of dry, oxygen-free nitrogen. Technical grade solvents were purified by standard procedures. The complex [Os$_3$H$_2$(CO)$_{10}$] was prepared by the literature procedure [23]. 1,4-Diphenylbuta-1,3-diyne and Me$_3$NO were used as obtained, without purification. Infrared spectra were recorded as dichloromethane solutions in NaCl cell (0.5 mm path length) on a Perkin–Elmer 1710 Fourier Transform spectrometer. FAB mass spectra were recorded on an AE1/Kratos MS 50 spectrometer. NMR spectra were recorded on a Bruker AM 400 Fourier Transform spectrometers and Bruker AM 500 instrument in appropriate solvents using Cr(acac)$_3$ as relaxation agent in the case of ^{13}C spectra. The chemical shifts were referenced to residual protons in CDCl$_3$ (7.25 ppm) for ^{1}H and to CDCl$_3$ (77.0 ppm) for ^{13}C.

3.1. Preparation of [Os$_3$(μ-H)(CO)$_{10}${μ$_3$-η^1:η^3:η^1-Ph(C)C$_9$H$_6$)}] (1 and 2)

[Os$_3$H$_2$(CO)$_{10}$] (90 mg, 0.11 mmol) was dissolved and magnetically stirred in CH$_2$Cl$_2$. 1,4-Diphenylbuta-1,3-diyne (25 mg, 0.12 mmol) was added to the solution and the mixture was stirred for 18 h. The resulting orange CH$_2$Cl$_2$ solution was evaporated to dryness under reduced pressure. The crude products were separated on TLC plates using hexane–dichloromethane (6:1) as eluant, affording the major product **1** (high R_f) as a yellow air-stable solid (50%) and the minor product **2** (low R_f) as an orange, air-stable oily solid (25%). Both were recrystallised from a CH$_2$Cl$_2$–hexane solution, affording yellow air-stable blocks of **1a** and **2**. Crystallisation of **1** from chloroform–heptane solution at -5 °C gave the **1b** crystalline form of **1**. Small amounts of the known complex [Os$_3$(CO)$_{10}${PhC$_2$C$_2$Ph}] (**5**) (10%) were also obtained upon purification and characterised by comparison with spectroscopic data obtained from the literature.

3.2. Kinetics of the [Os$_3$H$_2$(CO)$_{10}$] reaction with PhC$_2$C$_2$Ph in CD$_2$Cl$_2$

A solution of [Os$_3$H$_2$(CO)$_{10}$] and PhC$_2$C$_2$Ph (mole ratio 1/4) was placed into NMR tube and the reaction course was monitored every 10 min measuring integral intensities of the hydride protons for [Os$_3$H$_2$(CO)$_{10}$] (-11.5 ppm), **1** (-16.8 ppm), **2** (-17.3 ppm). The data obtained were treated using a first order rate law. Accumulation of the non-hydrido complex [Os$_3$(CO)$_{10}$(PhC$_2$C$_2$Ph)] (**5**) was calculated as a difference between the starting cluster integral intensities and corresponding magnitudes of **1** and **2**.
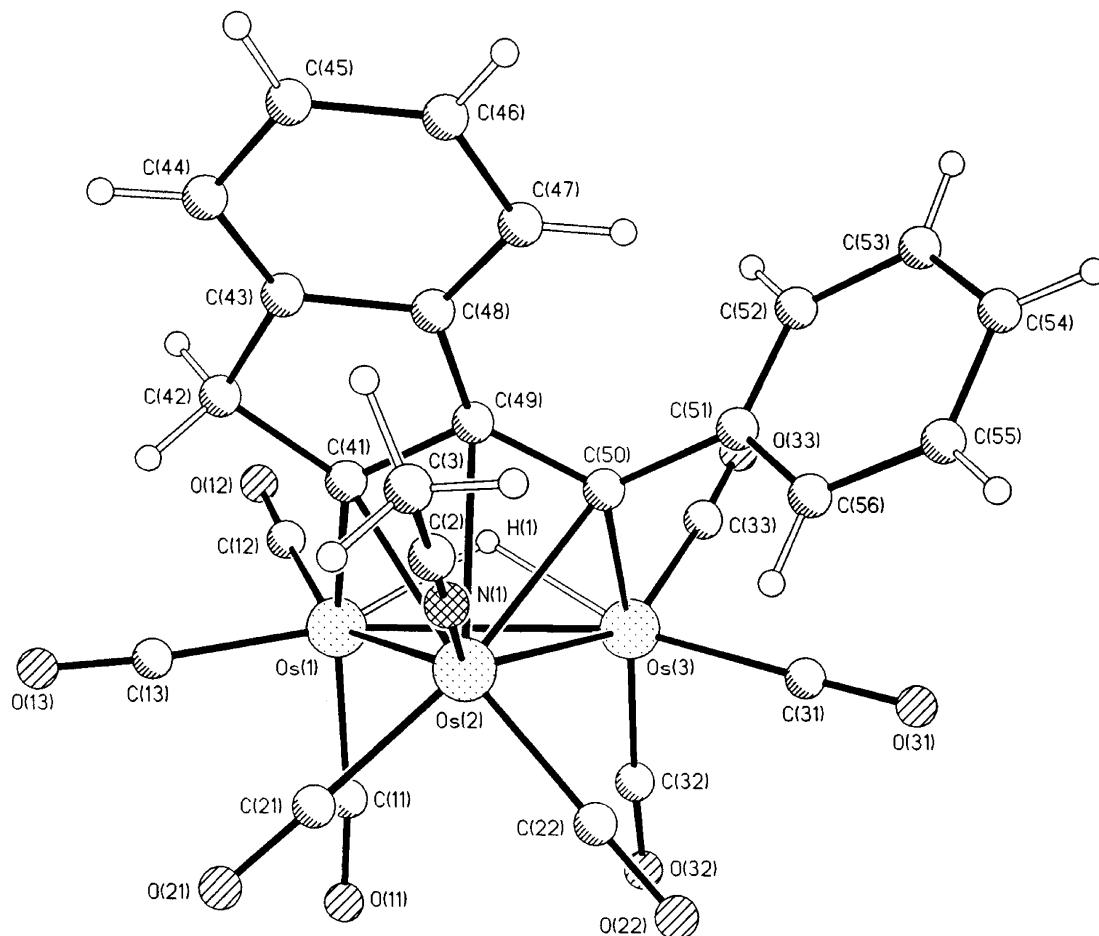
Fig. 4. The molecular structure of **4** showing the atom numbering scheme adopted.

3.3. Preparation of $[Os_3(\mu\text{-}H)(CO)_9\{\mu_3\text{-}\eta^1\text{:}\eta^3\text{:}\eta^1\text{-}Ph(C)C_9H_6)\}]$ (**3**)

The product **1** (50 mg, 0.047 mmol) was dissolved in heptane. The solution was refluxed for 3 h. The resulting yellow solution had the solvent removed under reduced pressure. The products were redissolved in a minimum of dichloromethane and separated on TLC plates using hexane as eluant, affording the **3** as a bright yellow air-stable solid (90%). Single crystals were grown from CHCl$_3$/heptane solution at +2 °C.

3.4. Preparation of $[Os_3(\mu\text{-}H)(CO)_8(MeCN)\{\mu_3\text{-}\eta^1\text{:}\eta^3\text{:}\eta^1\text{-}Ph(C)C_9H_6)\}]$ (**4**)

The product **1** (40 mg, 0.03 mmol) was dissolved in a CH$_2$Cl$_2$–acetonitrile mixture (1:1), that was cooled, and treated dropwise, with a 1.1 molar equivalent solution of Me$_3$NO (3.2 mg) in 5 cm^3 of CH$_2$Cl$_2$ over the period of 20 min. The solution then was stirred for 3 h, while being allowed to warm to room temperature, until it became pale yellow. The crude products were separated on TLC plates using hexane as eluant, affording **3** (high R_f) (ca. 40%, 12 mg) as a yellow air-stable solid, **4**, which

was isolated as an orange, air-stable solid in 40% yield (12 mg), and starting material **1** in 20% yield (at low R_f). Single crystals of **4** were grown from CH$_2$Cl$_2$–hexane solution.

3.5. Crystal structure determination of 1a, 2, 3 and 4

Data were collected by the $\omega/2\theta$ scan method on a Rigaku AFC5R (**1a**, **4**) four-circle diffractometer and by the ω/θ scan method on a Stoe-Siemens four-circle diffractometer (**3**). Semi-empirical absorption corrections based on ψ-scan data were applied to the data for, **1a**, **3** and **4** (TeXsan [24], SHELXTL-PLUS [25]). Data for **2** were collected on a Rigaku R-Axis IIc Imaging Plate (using $36 \times 5°$ oscillation frames) and processed using the BioteX package [24] with a semi-empirical absorption correction based on symmetry–equivalent reflections being applied.

The structures were solved by direct methods (heavy atom positions) and subsequent Fourier difference syntheses (SHELXTL-PLUS [25]) and refined anisotropically on all non-H atoms (**4**), Os and O atoms **2** or Os atoms alone **1a**, **3** by full-matrix least-squares on F^2 (SHELXL-93 [26]) with restraints to phenyl C–C dis-

Table 5[‡]

Complex	1a	2	3	4
Molecular formula	$C_{26}H_{12}O_{10}Os_3$	$C_{26}H_{12}O_{10}Os_3$	$C_{25}H_{12}O_9Os_3$	$C_{26}H_{15}NO_8Os_3$
M	1054.96	1054.96	1026.95	1039.99
Crystal system	Triclinic	Monoclinic	Triclinic	Triclinic
Space group	$P\bar{1}$	$P2_1/n$	$P\bar{1}$	$P\bar{1}$
a (Å)	14.284(8)	12.984(2)	10.6236(12)	13.899(2)
b (Å)	14.944(7)	11.791(2)	13.103(2)	11.217(2)
c (Å)	13.309(6)	18.110(3)	18.663(2)	8.6100(2)
α (°)	99.17(5)	90	94.380(10)	84.700(10)
β (°)	106.90(4)	103.180(10)	91.809(9)	101.550(10)
γ (°)	91.82(5)	90	97.088(7)	89.720(10)
U (Å^3)	2674(2)	2699.5(8)	2568.4(5)	1309.2(3)
Z	4	4	4	2
D_{calc} (Mg m^{-3})	2.620	2.596	2.656	2.638
Crystal size (mm)	$0.30 \times 0.25 \times 0.20$	$0.20 \times 0.12 \times 0.10$	$0.49 \times 0.42 \times 0.19$	$0.30 \times 0.30 \times 0.20$
Crystal habit	Yellow block	Yellow block	Yellow block	Yellow block
$F(0\,0\,0)$	1904	1904	1848	940
μ (mm^{-1})	14.274	14.141	14.856	14.57
Maximum, minimum relative transmission	1.00, 0.30	1.000, 0.242	0.164, 0.042	1.000, 0.686
Data collection range (°)	$1.62 < \theta < 27.64$	$1.76 < \theta < 21.97$	$3.53 < \theta < 22.49$	$2.5 < \theta < 25.0$
Index ranges	$0 \leq h \leq 18$, $-19 \leq k \leq 19$, $-17 \leq l \leq 16$	$-11 \leq h \leq 11$, $-14 \leq k \leq 14$, $-20 \leq l \leq 20$	$0 \leq h \leq 13$, $-12 \leq k \leq 12$, $-19 \leq l \leq 18$	$0 \leq h \leq 16$, $-13 \leq k \leq 13$, $-10 \leq l \leq 10$
Reflections measured	12 921	5688	12 188	4828
Independent reflections	12 421 ($R_{int} = 0.1291$)	3135 ($R_{int} = 0.0317$)	6554 ($R_{int} = 0.0381$)	4601 ($R_{int} = 0.047$)
Parameters, restraints	343, 30	222, 18	351, 74	332, 0
wR (all data)	0.3703 [a]	0.0729 [a]	0.1575 [a]	0.1084 [a]
x, y [a]	0.1217, 8.234	0.0193, 0	0.0855, 77.15	0.041, 10.81
$R_1[I > 2\sigma(I)]$ [a]	0.0735 [a]	0.0376 [a]	0.0483 [a]	0.0419 [a]
Observed reflections	6027	1685	5287	3388
Goodness-of-fit (all data)	1.041 [a]	0.995 [a]	1.016 [a]	1.016 [a]
Maximum shift (σ)	0.001	0.001	0.001	0.001
Peak, hole in final difference map (e Å^{-3})	3.979, −3.766	1.225, −1.366	1.984, −2.065	1.36, −1.51

[‡]Data in common: Graphite-monochromated Mo−K$_\alpha$ radiation, $\lambda = 0.71073$ Å, $T = 293(2)$ K, $R_1 = \Sigma||F_o|-|F_c||/\Sigma|F_o|$.

[a] $R_1 = \Sigma||F_o|-|F_c||/\Sigma|F_o|$, $wR_2 = [\Sigma(F_o^2-F_c^2)^2/\Sigma wF_o^4]^{1/2}$, $w = 1/[\sigma^2(F_o)^2+(xP)^2+yP]$, $P = (F_o^2-F_c^2)/3$, where x and y are constants adjusted by the program; Goodness-of-fit $= [\Sigma[w(F_o^2-F_c^2)^2/(n-P)]^{1/2}$ where n is the number of reflections and p the number of parameters.

tances in **1a** and **2**. In the final cycles of refinement a weighting scheme was introduced which produced a flat analysis of variance. Hydrogen atoms of the carbon ligand were placed in geometrically idealised positions and refined using a riding model; the bridging hydride ligands were located by a potential-energy minimisation method (HYDEX [19]) (**1a**, **3**, **4**) or from the final difference electron density map (**2**) and included in the final refinement cycles with coordinates and thermal parameters fixed. Crystal data and refinement details are summarised in Table 5.

4. Supplementary material

Crystallographic data (excluding structure factors) for the structures **1**, **2**, **3** and **4** have been deposited with the Cambridge Crystallographic Data centre, CCDC nos. 207009, 207010, 207011 and 207012, respectively. Copies of this information may be obtained free of charge from

The Director, CCDC, 12 Union Road, Cambridge CB2 1EZ, UK (fax: +44-1223-336033; e-mail: deposit@ ccdc.cam.ac.uk or www: http://www.ccdc.cam.ac.uk).

References

[1] P.J. Low, M.I. Bruce, Adv. Organomet. Chem. 48 (2002) 71.
[2] M. Tachikawa, J.R. Shapley, C.J. Pierpont, J. Am. Chem. Soc. 977 (1975) 172.
[3] A.J. Deeming, S. Hasso, M. Underhill, J.Chem. Soc. Dalton Trans. (1975) 1614.

[4] B.F.G. Johnson, R. Khattar, J. Lewis, P.R. Raithby, J. Organomet. Chem. 335 (1987) C17.

[5] B.F.G. Johnson, R. Khattar, F.J. Lahoz, J. Lewis, P.R. Raithby, J. Organomet. Chem. 319 (1987) C51.

[6] (a) G.A. Vaglio, O. Gambino, R.P. Farrari, G. Cetini, Inorg. Chim. Acta 7 (1973) 193;
(b) G.A. Vaglio, O. Gambino, R.P. Farrari, M. Chinone, Inorg. Chim. Acta 12 (1975) 155;
(c) G.A. Vaglio, O. Gambino, R.P. Farrari, G. Cetini, J. Organomet. Chem. 30 (1971) 381;
(d) G.A. Vaglio, O. Gambino, R.P. Farrari, M. Valle, G. Cetini, J. Chem. Soc. Dalton Trans. (1972) 1998.

[7] B.F.G. Johnson, R. Khattar, J. Lewis, P.R. Raithby, D.N. Smit, J. Chem. Soc. Dalton Trans. (1988) 1421.

[8] M.G. Karpov, S.P. Tunik, V.R. Denisov, G.L. Starova, A.B. Niko'skii, F.M. Dolgushin, A.I. Yanovsky, Yu. T. Struchkov, J. Organomet. Chem. 485 (1995) 219.

[9] (a) M.I. Bruce, P.J. Low, A. Werth, B.W. Skelton, A.H. White, J. Chem. Soc. Dalton Trans. (1996) 1551;
(b) L.P. Clarke, J.E. Davies, P.R. Raithby, G.P. Shields, J. Chem. Soc. Dalton Trans. (1996) 4147;
(c) A.J. Amoroso, L.P. Clarke, J.E. Davies, J. Lewis, H.R. Powell, P.R. Raithby, G.P. Shields, J. Organomet. Chem. 635 (2001) 119.

[10] R.D. Adams, BoQu, M.D. Smith, Organometallics 21 (2002) 4847.

[11] L.P. Clarke, J.E. Davies, P.R. Raithby, M.-A. Rennie, G.P. Shields, E. Sparr, J. Organomet. Chem. 609 (2000) 169.

[12] (a) A.J. Deeming, M.S.B. Felix, P.A. Bates, M.B. Hursthouse, J. Chem. Soc. Dalton Trans. 0 (1987) 461;
(b) A.J. Deeming, M.S.B. Felix, D. Nuel, Inorg. Chim. Acta 213 (1993) 3.

[13] S.P. Tunik, V.D. Khripun, I.A. Balova, E. Nordlander, M. Haukka, T.A. Pakkanen, P.R. Raithby, Organometallics 20 (2001) 3854.

[14] (a) N. Pirio, D. Touchard, L. Troupet, P.H. Dixneuf, J. Chem. Soc. Chem. Commun. (1991) 980;
(b) D. Touchard, N. Pirio, L. Troupet, M. Fettouhi, L. Ouahab, P. Dixneuf, Organometallics 14 (1995) 5263;
(c) M.I. Bruce, B.W. Skelton, A.H. White, N.N. Zaitseva, Inorg. Chem. Commun. 2 (1999) 17;
(d) L.P. Clarke, J.E. Davies, P.R. Raithby, G.P. Shields, J. Chem. Soc. Dalton Trans. (2000) 4527;
(e) M.I. Bruce, B.W. Skelton, A.H. White, N.N. Zaitseva, J. Clust. Sci. 13 (2002) 235.

[15] C.R. Pierpoint, Inorg. Chem. 16 (1977) 636.

[16] M.I. Bruce, B.W. Skelton, A.H. White, N.N. Zaitseva, Aust. J. Chem. 49 (1996) 155.

[17] C.M. Jensen, C.B. Knobler, H.D. Kaesz, J. Am. Chem. Soc. 106 (1984) 5926.

[18] S.L. Bassner, G.L. Geoffroy, A.L. Rheingold, Polyhedron 7 (1988) 791.

[19] A.G. Orpen, J. Chem. Soc. Dalton Trans. (1980) 2509.

[20] A.J. Deeming, Adv. Organomet. Chem. 26 (1986) 1 (and references therein).

[21] (a) A.D. Clauss, M. Tachikawa, J.R. Shapley, C.J. Pierpont, Inorg. Chem. 20 (1981) 1528;
(b) E. Sappa, A. Tiripicchio, A.M.M. Lanfredi, J. Organomet. Chem. 249 (1983) 391;
(c) A.G. Orpen, A.V. Riera, E.G. Bryan, D. Pippard, G.M. Sheldrick, K.D. Rose, J. Chem. Soc. Chem. Comm. (1978) 713;
(d) J.J. Guy, B.E. Reichert, G.M. Sheldrick, Acta Crystallogr. B32 (1976) 3319.

[22] P.A. Dawson, B.F.G. Johnson, J. Lewis, J. Puga, P.R. Raithby, M.J. Rosales, J. Chem. Soc. Dalton Trans. (1982) 233.

[23] H.D. Kaesz, S.A.R. Knox, J.W. Koepke, R.B. Saillant, J. Chem. Soc. Chem. Comm. (1971) 477.

[24] TeXsan, BioTex, Molecular Structure Corporation, 3200 Research Forest Drive, The Woodlands, TX, 77381, USA.

[25] SHELXTL-PLUS, PC Release 4.0, Siemens Analytical X-Ray Instruments Inc., Madison, WI, 1990.

[26] G.M. Sheldrick, SHELXTL-93, University of Göttingen, 1993.